

Emergent Criticality from Co-evolution in Random Boolean Networks

Min Liu* and Kevin E. Bassler†

Department of Physics, University of Houston, Houston, TX 77204-5005

(Dated: December 2, 2024)

The co-evolution of network topology and dynamics is studied in an evolutionary Boolean network model that is a simple model of gene regulatory network. We find that a critical state emerges spontaneously resulting from interplay between topology and dynamics during the evolution. The final evolved state is shown to be independent of initial conditions. The network appears to be driven to a random Boolean network with uniform in-degree of two in the large network limit. However, for biologically realized network sizes, significant finite-size effects are observed including a broad in-degree distribution and an average in-degree connections between two and three. These results may be important for explaining properties of gene regulatory networks.

PACS numbers: 87.23.Kg, 89.75.Hc, 05.65.+b, 87.15.Aa

I. INTRODUCTION

Boolean networks[1, 2, 3, 4, 5, 6, 7, 8] have been extensively studied over the past three decades. They have applications as models of gene regulatory networks, and also as models of social and economic systems. Boolean networks are defined as complex networks in which each node i has a Boolean dynamical state that is determined by input the node receives from K_i other nodes. As models of gene regulatory networks in cells, each node represents a gene whose Boolean state indicates whether or not it is being expressed, each dynamical attractor corresponds to a cell type, and the period of an attractor represents the period of its cell cycle. Despite the simplicity of Boolean networks, they capture the essence of many aspects of gene regulation and show rich and complex dynamics.

Perhaps the simplest Boolean network model is a homogeneous random Boolean network (RBN) in which each node has a same number of input nodes. In this case, the connections between nodes is described by a random directed graph $G(N, K)$ consisting of N nodes with uniform in-degree K . Figure 1 illustrates an example of $G(7, 3)$. As the parameters of homogeneous RBN model are varied, two phases of dynamical behavior, ordered and chaotic, are found[9, 10]. Between them there exists a narrow critical regime where the number of non-frozen and relevant nodes scales as a power-law with the size of the network[11, 12]. It has been argued[13, 14] that the regulatory networks of living systems should be at or close to criticality, at the so-called “edge of chaos,” because then they can maintain both the evolvability and stability. Studies of critical homogeneous RBNs have found that they exhibit some features of biological cells, including robustness against external perturbation analogous to homeostatic stability[15].

Accumulating experimental evidence[16, 17, 18, 19],

however, shows that real genetic networks do not have homogeneous connectivity, but, instead, are heterogeneous in topology. This diversity of architecture is, presumably, of great importance for the stability of living cells. Studies of random Boolean networks (RBNs) with heterogeneous topology have analytically determined the location of the ordered to chaotic phase transition for general RBNs in the large network limit[20, 21]. Also, in a related study, it has been found that for RBNs with power-law distributed connectivity the location of the phase transition from ordered to chaotic can be calculated as a function of the exponent of the power law describing the network topology [22, 23]. Both of these studies emphasized the importance of criticality and the influence of the network’s topology on its dynamics. However, they did not attempt to explain the evolution of critical networks with heterogeneous topology.

Several models have been proposed for evolutionary Boolean networks[24, 25, 26, 27, 28]. Of particular note is the work of Bornholdt and Röhl[27] who studied a random network model in which the nodes “fire” if the number of their positive binary inputs exceeds a threshold value. Their, so-called, threshold networks are then rewired based on how often nodes fire during the attractors. They found that the random threshold networks evolved to a critical network with average connectivity $\bar{K} = 2$ in the limit of large networks. Also, Luque *et al.*[28], studied a RBN model in which the topology of the network and the Boolean functions of the individual nodes evolved with a threshold rule related to the Bak-Tang-Weisenfeld sandpile model[29, 30]. They found that with their model the networks evolved to self-organized critical RBNs. However, the topology of the network in the evolved state, other than the average connectivity, was not studied.

Here, we present a study of an evolutionary RBN model that, independent of the initial topology of the network, evolves to a critical network with a finite number of nodes and which has a heterogeneous topology. This work is motivated in part by the studies described above as well as the recent experimental demonstration in *S. cerevisiae* [18] that transcription factors are able

*Electronic address: mliu3@uh.edu

†Electronic address: bassler@uh.edu

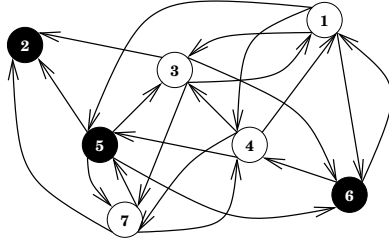


FIG. 1: A directed graph $G(7,3)$ represents a homogeneous RBN with 7 nodes and in-degree connectivity of 3. Black and white represent binary states ‘1’ and ‘0’ respectively. The state vector of network is $\Sigma(t) = (0, 1, 0, 0, 1, 1, 0)$. The arrow on each link indicates the direction of information flow in the network.

to alter their interactions to varying degrees in response to diverse stimuli thereby changing the topology of gene regulatory network. In the model we present, the evolutionary changes of the topology of the network are driven by the dynamics of the network, and the functions that control the dynamics of network simultaneously evolve due to the changes in the network topology. Thus, this study investigates the co-evolution of network topology and dynamics.

Two different variants of our model are considered, and our principal conclusions are the same for both of them. Perhaps our most important result concerns the finite-size effects of the model. As the size of the network increases, the distribution of in-degree connectivity becomes increasingly narrow and sharply peaked at a value of $K = 2$. However, for biologically realized network sizes, we show that the final evolved critical state has a broad distribution of in-degree connectivity with an average value between 2 and 3. Both of these features also occur in real networks, suggesting that many of the topological features of real networks may be due to their finite size.

II. DEFINITION OF MODEL

A. Dynamics of Random Boolean Networks

A generalized RBN consists of N randomly interconnected nodes, $i = 1, \dots, N$, each of which has K_i in-degree connections from nodes that regulate its behavior. Each node has a Boolean dynamical state at time t , $\sigma_i(t) = 0$ or 1. The state of each node at time $t + 1$ is a function of all states of its K_i regulatory nodes at time t . Hence, the discrete dynamics of the network is given by

$$\sigma_i(t + 1) = f_i(\sigma_{i_1}(t), \sigma_{i_2}(t), \dots, \sigma_{i_{K_i}}(t)) \quad (1)$$

where i_1, i_2, \dots, i_{K_i} are those input nodes regulating node i . The function f_i is a Boolean function of K_i variables that determines the output of node i for all of the 2^{K_i}

possible sets of input. The functions are randomly generated with the interaction bias p , which is the probability for the output value to be 1 for each set of input. The bias p can be interpreted as a biochemical reaction parameter.

Given the Boolean state of each node i at time t , $\sigma_i(t)$, the state vector of network $\Sigma(t)$ is defined as the system state consisting of a sequence of binary numbers $(\sigma_1(t), \dots, \sigma_N(t))$. For instance, in Fig. 1, the state vector $\Sigma(t) = (0, 1, 0, 0, 1, 1, 0)$. The path that $\Sigma(t)$ takes over time t is a dynamical trajectory in the phase space of system. The phase space consists of 2^N possible system states. Thus, the phase space is finite for a finite number of nodes N . Due to this and the fact that the dynamics defined in Eq. 1 is deterministic, all dynamical trajectories must eventually become periodic. That is, after some possible transient behavior, each trajectory will repeat itself forming a cycle given by,

$$\Sigma(t) = \Sigma(t + \Gamma). \quad (2)$$

The periodic part of the trajectory is the attractor of the dynamics, and the minimum $\Gamma > 0$ that satisfies Eq. 2 is the period of the attractor.

In general, multiple attractors of different periods co-exist in the phase space. The initial state $\Sigma(0)$ determines which attractor the network finally reaches. The set of all initial states reaching the same attractor forms a basin in the phase space. Two phases exist in RBNs, chaotic and ordered, characterized by their dynamical behavior. One important way of characterizing the dynamical behavior of an RBN is to measure the distribution of its attractor periods beginning with random initial states. For RBNs in the chaotic phase the distribution of attractor periods is sharply peaked near an average value that grows exponentially with system size N , and for RBNs in the ordered phase the distribution of attractor periods is sharply peaked near an average value that is nearly independent of N . Critical RBNs, however, have a broad power law distribution of attractor periods[15].

B. Co-evolution in Random Boolean Networks

Here we study the co-evolution of network topology and dynamics in a model in which topology is changed due to a local rewiring rule that is a function of network dynamics. Similar to the one used in Ref. [27], the rule is simply that a frozen gene grows a link while an active gene loses a link. The dynamical functions can be changed in either an annealed or a quenched way. The detailed algorithm is defined as follows:

1. Start with a homogeneous RBN. Choose a random directed network $G(N, K_0)$ with uniform in-degree connectivity $K_i = K_0$ for all N , and generate a random Boolean function f_i for each node i using an interaction bias $p = 0.5$.

2. Choose a random initial system state $\Sigma(0)$. Update the state using Eq. 1 and find the dynamical attractor. See the appendix for a description of the algorithm used to find the attractor.
3. Choose a node i at random and determine its average output state $\overline{O}(i)$ over the attractor.

$$\overline{O}(i) = \frac{1}{\Gamma} \sum_{t=T}^{T+\Gamma-1} \sigma_i(t) \quad (3)$$

where T is a time large enough so that the periodic attractor has been reached, and Γ is the period of the attractor. If $\overline{O}(i) = 1$ or 0 , then its state does not change over the duration of the attractor; it is frozen. Alternatively, if $0 < \overline{O}(i) < 1$, then node i is active during the attractor.

4. Change the network topology by rewiring the connections to the node chosen in the previous step. If it is frozen, then a new incoming link from a randomly selected node j is added to it. If it is active, then one of its existing links is randomly selected and removed. Note that this rewiring changes K_i .
5. The Boolean functions of network are regenerated. Two different methods have been used:
 - Annealed model: A new Boolean function is generated for every node of the network.
 - Quenched model: A new Boolean function is generated only for the chosen node i , while the others remain what they were previously.

In both cases all new functions are generated with an interaction bias $p = 0.5$.

6. Return to step 2.

The time scale for an evolutionary change of the networks, steps 2 – 6 above, is called an epoch.

As we will see, using this rewiring rule the network topology evolves from a homogeneous one to a heterogeneous one. Note that by this rule the evolution of the network topology is driven by the network dynamics. At the same time, the functions that control the network dynamics evolve as network topology changes. Thus there is feedback between the evolution of topology and the evolution of dynamics.

III. SIMULATION AND RESULTS

We have simulated both the annealed and the quenched variants of the model. Both variants give very similar results, and our principal findings are the same for both variants. Therefore, we will present here mainly results from the annealed variant. Graph (a) of Fig. 2 shows the evolution of the average in-degree connectivity $\overline{K} = \frac{1}{N} \sum_{i=1}^N K_i$ for networks of size $N = 30$ in the

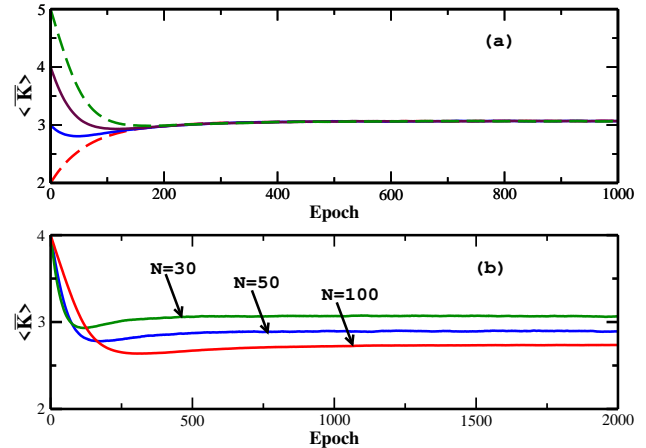


FIG. 2: (a). Evolution of the ensemble averaged in-degree connectivity in the annealed model for networks of size $N = 30$. The networks in each ensemble initially start from different uniform connectivity, $K_0 = 2, 3, 4$, and 5 , but reach a same statistical steady state $\langle \overline{K} \rangle = 3.06$. Each ensemble contained 15,000 realizations of the network. (b). Evolution of ensemble averaged in-degree connectivity for networks of three different size $N = 30, 50$, and 100 in the annealed model.

annealed variant of the model. Four curves are shown. They show the results obtained by beginning with networks with different uniform connectivity $K_0 = 2, 3, 4$, and 5 . Each curve is the average of 15,000 independent realizations of the network evolution. This ensemble average is indicated by the angular brackets. Each different realization in an ensemble begins with a different random network and with a different random initial state vector. Remarkably, despite the difference in initial conditions, all four curves collapse after about 200 epochs, and they all approach the same final statistical steady state that has an average in-degree connectivity $\langle \overline{K} \rangle = 3.06$. This occurs without tuning and suggests that the final evolved topology of the network is independent of the initial topology of the network. The steady state value of $\langle \overline{K} \rangle$ depends on the size of the system as shown in graph (b) of Fig. 2. Starting with networks that all have the same initial uniform connectivity $K_0 = 4$, but which have different size $N = 30, 50$, and 100 , we find that larger networks evolve to steady states with smaller values of $\langle \overline{K} \rangle$. Very similar results are obtained for the quenched version of the model. For example, for networks with $N = 30$ the steady state value of the average connectivity is $\langle \overline{K} \rangle = 3.08$.

We have also calculated the in-degree and out-degree connectivity distributions, $P(K_{in})$ and $P(K_{out})$, of the evolved RBNs in the steady state. Initially, all nodes of the network have a uniform in-degree K_0 , meaning that the in-degree distribution is a discrete delta function $P(K_{in}) = \delta_{K_{in}, K_0}$, and the out-degree distribution is a binomial distribution. However, through the evolutionary rewiring of the network both the in-degree and out-degree distributions change. The in-degree and out-

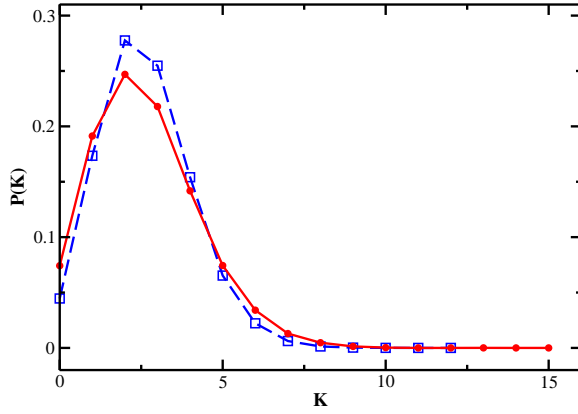


FIG. 3: Distribution of in-degree (square) and out-degree (circle) connectivity in the annealed model. The size of the networks is $N = 200$.

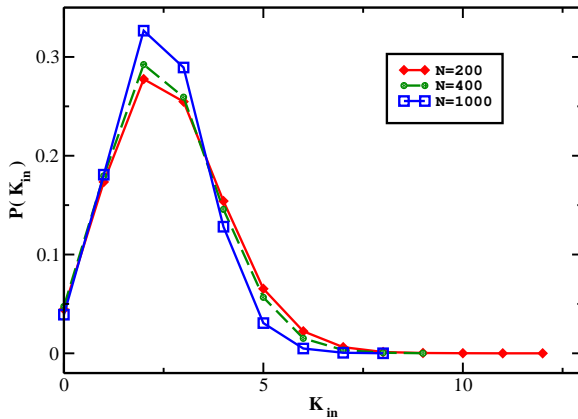


FIG. 4: Distribution of in-degree connectivity in the annealed model. The network sizes are $N = 200, 400$, and 1000 .

degree distributions in the steady state of the annealed version, are shown in Fig. 3 for $N = 200$. They are both right skewed bell-shaped distributions peaking at $K = 2$. The out-degree distribution remains a binomial distribution but the average connectivity changes. The in-degree distribution, although it has the same average connectivity as the out-degree distribution, is more sharply peaked. As the size of the network grows, the in-degree distribution becomes increasingly narrow and peaked at the value $K_{in} = 2$, as shown in Fig. 4. Based on this observation, we conjecture that the distribution tends to converge into a discrete delta function $\delta_{K_{in},2}$ in the large network limit $N \rightarrow \infty$, indicating that the network becomes a homogeneous RBN in that limit.

In order to probe the dynamical nature of evolved steady states we computed the distribution $P(\Gamma)$ of steady state attractor period Γ in the ensemble of RBNs simulated. The distribution has a broad, power-law behavior for both the annealed and quenched variants of the model. Figure 5 shows the results for networks with

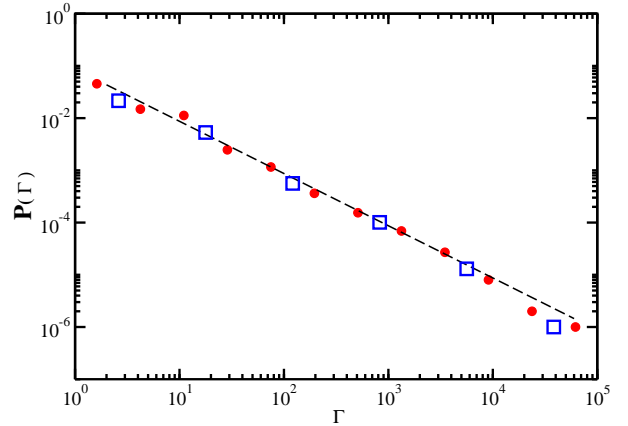


FIG. 5: Power law distribution of steady state attractor period Γ in both annealed (circle) and quenched (square) models for $N = 200$ system. The dashed straight line has a slope of 1.0.

$N = 200$. As long as N is about 30 or larger, results for other size networks are similar. As discussed above, this power-law distribution indicates that the networks have critical dynamics. Also in the figure, the straight line has a slope of 1.0. Thus, the critical exponent describing the power-law is approximately 1.0. This value of the exponent is obtained for all system sizes studied in both the quenched and annealed versions of the model. In short, we find that a robust criticality emerges in the evolutionary random Boolean networks.

Given the steady state value $\langle \bar{K} \rangle = 2$ in the large network limit $N \rightarrow \infty$, we studied the finite-size effects in the model. As shown in Fig. 6, the values of $\langle \bar{K}(N) \rangle$ for finite N obey the scaling function

$$\langle \bar{K}(N) \rangle - 2 = AN^{-\beta}. \quad (4)$$

Fitting the data to this function, we find that the coefficient is $A = 2.50 \pm 0.06$ and the exponent is $\beta = 0.264 \pm 0.005$. Thus the value of $\langle \bar{K}(N) \rangle$ is always larger than 2 for finite N . Note that steady state values of the average connectivity in random threshold networks have a similar scaling form [27], but, in that case $A = 12.4 \pm 0.5$ and $\beta = 0.47 \pm 0.01$.

IV. DISCUSSION AND CONCLUSIONS

The mechanism we find here that leads to the emergent critical state has some similarity to self-organized criticality (SOC)[29, 30], but is different. SOC is the tendency of driven dissipative dynamical systems to organize themselves into a critical state far from equilibrium through avalanches of activity of all sizes. In our particular model, the evolutionary Boolean network is a dissipative dynamical system because multiple different states may map into the same attractor so that information is lost. Similar to SOC systems, our model is driven subject

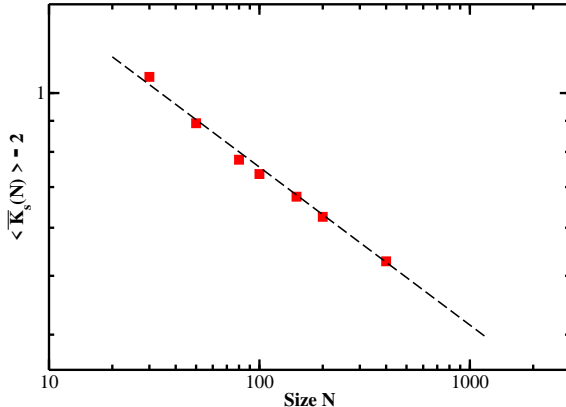


FIG. 6: Finite-size effects in the annealed model. The data shown are for systems of different sizes $N = 30, 50, 80, 100, 150, 200$, and 400 . The dashed straight line has a slope of 0.26 .

to two competing rules, and the network organizes itself into a steady state that results from a dynamical balance of the competition between those rules. Moreover, the critical state is robust irrespective of initial connectivity in both the quenched or annealed versions of the model. The emergent critical state acts like a global attractor in the evolution process. However, unlike the mechanism of traditional SOC, but similar to the mechanisms that have been shown to lead to criticality in random threshold networks [27] and in homogeneous Boolean networks [24], the self-organizing mechanism here is based on a topological phase transition in dynamical networks.

Our results indicate that, with the rewiring rules we use, networks in the limit $N \rightarrow \infty$ will evolve to have a homogeneous in-degree connectivity of 2. However, we find that finite size networks evolve to have a broadly distributed heterogeneous in-degree connectivity. The average in-degree connectivity of the evolved networks is between 2 and 3 for biologically realized network sizes. This result may be important for explaining the observed structure of real gene regulatory networks. Real genetic networks have a number of nodes N ranging from near 100 to thousands, and typically have a heterogeneous connectivity with an average in-degree slightly larger than 2. For example, a recent experiment studying the gene regulatory network of *S. cerevisiae* [18] found that the network contains 3420 genes and has an average in-degree connectivity $\bar{K}_{in} = 2.1$.

Finally, we note that real genetic networks exhibit an approximately scale-free out-degree distribution while the in-degree distribution is exponentially decaying[18]. In our numerical study, we similarly obtain an in-degree distribution that decays faster than the out-degree distribution, but our model does not produce a scale-free like out-degree distribution. Therefore, in order to be more realistic the model needs to be extended by adding other factors that will capture this feature. We do not believe though that such extensions will alter the principal con-

clusions of this paper concerning the importance of finite size effects in the evolution of network topology in real genetic networks.

Acknowledgments

We thank Maximino Aldana, Julio Monte, Toshimori Kitami and Adam Sheya for stimulating discussions. This work was supported by the NSF through grant #DMR-0427538, and by SI International through the AFRL under contract #FA8756-04-C-0258.

*

APPENDIX A

Finding the dynamical attractor of a Boolean network can be computationally challenging. In the work presented here and in previous studies of our group[24, 25, 26] the following algorithm was used to determine the attractor.

We begin by using the initial state $\Sigma(0)$ as the ‘‘checkpoint’’ state. Then for each time T , $0 < T \leq T_1$, the state is updated using Eq. 1. After each update the new state $\Sigma(T)$ is compared to the initial state. If the two states are the same, then the attractor is found, it has period T , and the search ends. Note that the new state is compared only to the checkpoint state and no other previous states.

If after T_1 updates no attractor is found then the state $\Sigma(T_1)$ is used as the new checkpoint state. For each time T , $T_1 < T \leq T_2$, the state is again updated using Eq. 1. After each update the new state $\Sigma(T)$ is compared to the checkpoint state. If the two states are the same, then the attractor is found, it has period $T - T_1$, and the search ends.

If after T_2 updates the attractor has still not been found then the state $\Sigma(T_2)$ is used as the new checkpoint state. For each time T , $T_2 < T \leq T_2 + T_{max}$, the state is again updated using Eq. 1. After each update the new state $\Sigma(T)$ is compared to the checkpoint state. If the two states are the same, then the attractor is found, it has period $T - T_2$, and the search ends.

Finally, if after $T_2 + T_{max}$ updates the attractor has still not been found then the state $\Sigma(T_2 + T_{max})$ is used as the new checkpoint state. Once again after each update, $T_2 + T_{max} < T \leq T_2 + 2T_{max}$, the new state is compared to the checkpoint state. If the two states are the same, then the attractor is found, it has period $T - T_2 - T_{max}$, and the search ends.

If no attractor is found after this procedure, then we stop. In this case, the average output state in Eq. 3 is calculated assuming that the attractor period is $\Gamma = T_{max}$ and that the final checkpoint state $\Sigma(T_2 + T_{max})$ is on the attractor.

This algorithm finds all attractors that have period less than or equal to T_{max} and that have a transient time

to reach the attractor from the initial state less than or equal to $T_2 + T_{max}$. For the results presented in this

paper we used $T_1 = 100$, $T_2 = 1000$, and $T_{max} = 100000$.

[1] M. Aldana, S. Coppersmith, and L. P. Kadanoff, in *Perspectives and Problems in Nonlinear Science*, edited by E. Kaplan, J.E. Marsden, and K.R. Sreenivasan (Springer-Verleg, Berlin, 2003).

[2] S. A. Kauffman, *J. Theor. Biol.* **22**, 437 (1969).

[3] S. A. Kauffman, *Physica D* **42**, 135 (1990).

[4] R. Albert and A. L. Barabási, *Phys. Rev. Lett.* **84**, 5660 (2000).

[5] U. Bastolla and G. Parisi, *Physica D* **115**, 203 (1998).

[6] F. Greil and B. Drossel, *Phys. Rev. Lett.* **95**, 048701 (2005).

[7] B. Drossel, *Phys. Rev. E* **72**, 016110 (2005).

[8] B. Drossel, T. Mihaljev, and F. Greil, *Phys. Rev. Lett.* **94**, 088701 (2005).

[9] B. Derrida and Y. Pomeau, *EuroPhys. Lett.* **1**, 45 (1986).

[10] B. Derrida and G. Weisbuch, *J. Phys.* **47**, 1297 (1986).

[11] J. E. S. Socolar and S. A. Kauffman, *Phys. Rev. Lett.* **90**, 068702 (2003).

[12] V. Kaufman, T. Mihaljev, and B. Drossel, *Phys. Rev. E* **72**, 046124 (2005).

[13] N. H. Packard, in *Dynamics Patterns in Complex Systems* (World Scientific, Singapore, 1988).

[14] S. A. Kauffman, *The Origins of Order* (Oxford University Press, New York, 1993).

[15] U. Bastolla and G. Parisi, *J. Theor. Biol.* **187**, 117 (1997).

[16] D. Thieffry, A. M. Huerta, E. Perez-Rueda, and J. Collado-Vides, *Bioessays* **20**, 433 (1998).

[17] T. I. Lee, N. J. Rinaldi, F. Robert, D. T. Odom, and Z. B. J. *et al.*, *Science* **298**, 799 (2002).

[18] N. M. Luscombe, M. M. Babu, H. Yu, M. Snyder, and S. A. T. M. Gerstein, *Nature* **431**, 308 (2004).

[19] A. H. Y. Tong, G. Lesage, G. D. Bader, H. Ding, and H. X. *et al.*, *Science* **303**, 808 (2004).

[20] B. Luque and R. V. Solé, *Phys. Rev. E* **55**, 257 (1997).

[21] J. J. Fox and C. C. Hill, *Chaos* **11**, 809 (2001).

[22] M. Aldana, *Physica D* **185**, 45 (2003).

[23] M. Aldana and P. Cluzel, *Proc. of the Natl. Acad. Sci. U.S.A.* **100**, 8710 (2003).

[24] M. Paczuski, K. E. Bassler, and A. Corral, *Phys. Rev. Lett.* **84**, 3185 (2000).

[25] K. E. Bassler, C. Lee, and Y. Lee, *Phys. Rev. Lett.* **93**, 038101 (2004).

[26] K. E. Bassler and M. Liu, in *Noise in Complex Systems and Stochastic Dynamics III, Proc. of SPIE Vol. 5845*, edited by L. B. Kish, K. Lindenberg, and Z. Gingl (SPIE, Bellingham, WA, 2005), P. 104.

[27] S. Bornholdt and T. Röhl, *Phys. Rev. Lett.* **84**, 6114 (2000).

[28] B. Luque, F. J. Ballesteros, and E. M. Muro, *Phys. Rev. E* **63**, 051913 (2001).

[29] P. Bak, C. Tang, and K. Wiesenfeld, *Phys. Rev. Lett.* **59**, 381 (1987).

[30] P. Bak, C. Tang, and K. Wiesenfeld, *Phys. Rev. A* **38**, 364 (1988).